INTRASEASONAL VARIABILITY IN THE EQUATORIAL PACIFIC

Interim Report

Hans von Storch
Max-Planck-Institut für Meteorologie, Hamburg

ABSTRACT

Daily data of atmospheric and oceanic data from the equatorial Pacific are analysed.

Associated correlation patterns, which are linked to an index of the *Madden and Julian Oscillation* (MJO), of local buoy data and of tropical low level wind analysis are derived. The zonal *wind signal* associated with the MJO is of global scale with a zonal wave number 1 pattern. Typical wind anomalies are of the order of 1.5 m/s. The rotation of the wind is anti-clockwise in the western Pacific (165°E) but clockwise in the eastern Pacific (140°W). The wind signal is estimated to propagate with a phase speed of about 12 m/s. The *thermocline depth signal* is of the order of 2m in the west and 4m in the east. The phase speed is estimated to be about 4 m/s.

The 6-dimensional vector of *thermocline depth and wind component at the 165°E and 140°W buoys* has been subjected to a *POP analysis*: One not too clearly defined signal is identified. It describes the eastward propagation of a fast signal (phase speed ≈ 5 m/s) in the atmosphere and a slow signal in the ocean (phase speed ≈ 2.5 m/s). The oceanic variability is maximum at 140°W and the atmospheric is strongest at 165°E. The transfer function between atmospheric and oceanic variability is very different at the two locations.

Apparently both approaches are successful in identifying only one of the two time scales correctly: the MJO-associated correlation patterns capture the atmospheric time scale but overestimates the oceanic phase speed considerably; the POP analysis of the buoy data yields a reasonable of the oceanic phase speed but also a strong underestimation of the atmospheric time scale. A stochastic vector model which is believed to resolve both the atmospheric and the oceanic time scales, is proposed.

1. INTRODUCTION

Two factors contribute to the intraseasonal variability in the equatorial ocean, namely the atmospheric forcing which is dominated by the eastward propagating Madden and Julian Oscillation (MJO; Madden and Julian, 1972; Madden, 1986; Lau etc, Weickmann etc) and the oceanic wave dynamics, in particular the eastward propagating equatorial Kelvin waves (Spillane et al., 1987; McPhaden and Taft. 1988). Interestingly, the two processes, MJO and oceanic Kelvin wave, have quit different time scales: That of the MJO is about 45 days whereas that of the Kelvin waves is of the order of few months.

In this study we attempt to describe the typical sequence of events that is associated with the passage of the MJO in the Pacific ocean. For that purpose a complex index of the MJO is used in order to derive associated correlation patterns of low level wind and buoy data. Also we analyze the joint variability in the coupled atmosphere-ocean system by means of a POP analysis of daily surface wind and 20°C isotherm depth at two equatorial locations.

2. DATA

Three sets of data are used:

(1) Daily reports of the zonal and meridional component of the surface (anemometer height) and of the depth of the 20° depth at two moored buoys located at 165°E and 140°W. Fairly complete records are available from May 1984 trough December 1989 for the 140°W buoy and from December 1987 until November 1989 for the 165°E. See Figure 1. The data were kindly provided by M. McPhaden of PMEL Seattle. (McPhaden and Taft, 1988; McPhaden et al., 1990; McPhaden and Hayes, 1990)

(2) A complex index ζ of the state of the MJO. This index is derived by means of a POP analysis of the intraseasonal variability of the equatorial velocity potential along the equator at 200 mb (Storch and Xu, 1990). The equatorial velocity potential MJO signal may be described by $z_1 p^1 + z_2 p^2$ with $\zeta = z_1 + iz_2$ and p^1 and p^2 shown in Figure 2. Being complex this index incorporates information on the phase and the strength of the MJO. It is available from May 1984 through April 1989. The POP analysis revealed a base period of about 45 days for the MJO and its index.

(3) Daily ECMWF analysis of zonal wind at 850 mb from May 1984 through April 1988.

3. The Signal Excited by the MJO

In this section we use the index of the MJO (Storch and Xu, 1990) to derive the typical evolution, parallel to the MJO, in other variables by means of the Associated Correlation Pattern Analysis (ACPA; Storch et al., 1988)). If $\zeta(t) = z_1(t)+iz_2(t)$ is the complex index of the MJO, two MJO-associated correlation patterns q_U^1 and q_U^2 for the parameter field U, e.g. the zonal wind at 850 mb, are obtained by minimizing $\langle \|U(t) - z_1'(t)q_U^1 - z_2'(t)q_U^2\|^2 \rangle$. The prime ' indicates a normalization of the time coefficients:

$$z_1' = z_1 / \sqrt{2\ \mathrm{Var}(z_1)}$$

This normalization deviates from that in Storch et al. (1988) by the factor $\sqrt{2}$. With the present normalization the associated pattern q_U^1 represents the typical state if $\zeta = z_1$ and, similarly, q_U^2 represents the typical state if $\zeta = iz_2$ (see Appendix). Or, the signal is equal to q_U^1 if $z_1^2 = \mathrm{Var}(z_1 | z_2=0)$. In contrast to that the normalization suggested by Storch et al. (1988) yields a pattern q_U^1 representative for the state if $z_1^2 = \mathrm{Var}(z_1)$.

The results have to be interpreted such that there is a tendency to observe the 2-patterns (of 200 mb velocity potential; 850 mb wind, surface wind at the buoys, depth of the 20°C isotherm) at the same time and the 1-patterns a quarter of the base period (45 days) later. After another quarter of the period, the negative 2-patterns will appear, then the negative 1-patterns and finally the 2/pattern again. Or, symbolically: $\ldots \rightarrow q_U^2 \rightarrow q_U^1 \rightarrow -q_U^2 \rightarrow -q_U^1 \rightarrow q_U^2 \rightarrow \ldots$

The basic signal in the equatorial 200mb velocity potential is given by the two patterns shown in Fig. 2: It describes the eastward propagation of a zonal wave number 1 pattern with a period of 45 days. It represents the MJO (Storch and Xu, 1990).

The minimization is done for all data ("all year"), or only for a subset of the data, namely (northern) summer ("MJJA") and winter ("NDJF").

The nature of the ACPA is the same as regression analysis. As such the signal identified with ACPA will have the same time scale as the controlling variable which is in this case the MJO index. Since the MJO time scales is about 45

days, the data have band pass filtered prior to the ACPA: variance on time scales between 30 and 90 days is unchanged, variability on times scales below 20 and above 150 days is completely removed. Between 20 and 30 days and between 90 and 150 days a cosine tapering is applied.

a) All year conditions

The percentage of band-pass filtered variance of 850 mb wind that may be explained by the MJO index has maximum values of up to 35% next to the equator: along the ITCZ, the Maritime Continent and the equatorial Indian Ocean (Fig. 3). The patterns are, consistently with the velocity potential patterns (Fig. 2), of zonal wave number 1 scale with low level convergence and upper level divergence at the minima of the velocity potential. Maximum winds in the associated correlation patterns are 1.5 m/s, which represents the typical strength of the band-pass filtered MJO signal.

The results for the surface winds and for the 20°C isotherm depth at the two buoy locations are given in the following table. The days are numbered so that pattern q^1 appears on day 0, q^2 at day 11.25, and so on.

Position	parameter	q^1	q^2	maximum at day	explained variance
165°E	u	0.82	-0.36	3	9%
	v	-0.28	-0.09	-2	6%
	z	1.7	-1.4	5	9%
140°W	u	0.12	-0.33	9	9%
	v	0.14	0.05	2	4%
	z	-4.6	-0.3	22	9%

The results for the winds are depicted graphically in Figure 4: The typical sequence of events is given as an ellipse, and the straight lines indicate the ACPs q_U^1 and q_U^2. Since the cycle is given by ... $\rightarrow q_U^2 \rightarrow q_U^1 \rightarrow -q_U^2 \rightarrow -q_U^1 \rightarrow q_U^2 \rightarrow$... the wind rotates anti-clockwise at 165°E but clockwise at 140°W. The zonal wind component is considerably stronger than the meridional wind component.

The buoy wind results are consistent with the ECMWF 850 mb wind analysis (Fig. 3): In the 2-pattern the wind anomalies at both locations are moderately easterly (typically about 0.5 m/s) and in the 1-pattern westerly wind anomalies prevail that are significant at 165°E (approximately 1 m/s) and very weak at 140°W. The percentage of variance explained by the MJO is less than 10% in these "all year" conditions.

If we adopt the notion that an idealized MJO is given by the cycles $\cos(\omega t)q^2 + \sin(\omega t)q^1$, with $\omega = 2\pi/45$ days, maximum zonal winds occur at 165°E at t = 3 days and at 140°W at t = 9 days (Fig. 4). Given a longitudinal distance of 55° or approximately 6100 km, the phase speed of the wind signal in the central Pacific is 12 m/s which is consistent with previously published estimates.

The signal in terms of the 20°C isotherm depth is shown in Figure 5 as the synthesized evolution, $\cos(\omega t)q^2 + \sin(\omega t)q^1$, at the two positions. The variations at the central Pacific positions are more energetic than those at the 165°E. The typical maximum anomaly in the western Pacific is only 2m whereas the one in the Central pacific is 4 m. In principle, there are two interpretations of Figure 5: The signal is propagating eastward, and a maximum at 165°E is observed at 140°W after about 17 days, or the signal is moving westward, and the delay is about 28 days. Since there are no physical arguments for the westward propagation, we interpret the signal as eastward propagating. The maximum deepening of the 165°E thermocline happens at t = 5 days, i.e. 2 days after the maximum local wind forcing. At 140°W, the maximum depth is at t = 22 days (Fig. 5), i.e., 17 days after the maximum at 165°E and 13 days after the maximum local wind. Thus its phase speed is estimated to be about 4.2 m/s.

This phase speed of 4.2 m/s is about twice the phase speed of the fastest baroclinic Kelvin wave which was estimated by McPhaden and Taft (1988) to be 1.7 to 2.2 m/s in the eastern equatorial Pacific. It is *not* consistent with a cross correlation analysis of the band-pass filtered z-data at the two positions shown in Figure 6: Maximum positive correlations are obtained for a lag of about 35 days with the 165°E data leading the 140°W data. A lag of 35 days corresponds to a phase speed of 2.0 m/s which is close to the theoretically derived phase speed of the fastest Kelvin wave. If this discrepancy is due to problems of the analysis scheme or if it is reflecting something real remains to be clarified. Note, however, that the ACPA does not directly relate the time series at the two positions, as the cross correlation does, but makes uses of the MJO index.

In summary, the ACPA of all data yields the following concept: Parallel to strong westerly wind anomalies (q^1_U) in the western Pacific, the thermocline tends to be slightly deeper in the west (1.5 m) but considerably shallower in

the east (5 m). A quarter of a period later, i.e., after 11 days, parallel to $-q_U^2$, there are still significant westerly wind anomalies in the western Pacific, and the thermocline at 140°W is quickly rising, and positive depth anomalies are present at both locations (1-2 m). After another 11 days and the Central Pacific thermocline has deepened by about 5 m. At the same time, however, strong easterly wind anomalies have arrived at the west Pacific location as the MJO passes by in its negative phase.

b) Northern winter (NDJF) conditions

The associated correlation patterns derived for NDJF zonal wind at 850 mb are shown in Figure 7. The signal is stronger than in the "all year" data set: Maximum winds are 2.5 m/s, and the two ACPs describe the signal to propagate from the South equatorial Indian Ocean (q^1) into the area of the SPCZ (q^2). Maximum percentages of explained variance are more than 40%.

The ACPs found for the buoy data are listed in the following table, the wind ellipses are shown in Fig. 4.

Position	parameter	q^1	q^2	maximum at day	explained variance
165°E	u	1.05	-1.03	5	16%
	v	-0.47	-0.14	20	11%
	z	2.5	-1.7	4	13%
140°W	u	0.10	-0.37	9	12%
	v	0.11	-0.01	1	2%
	z	-7.9	-0.5	22	21%

The orientation of the NDJF ellipses are fairly similar to the "all year" ellipses; at 165°E the winds are stronger. The phase speed for the zonal wind signal is 6100 km/4 days ≈ 18 m/s, which is 50% faster than in the "all year" case. One might speculate if this is due to the fact that the seasonal convectively active area is not along the equator but bent off into the SPCZ. It has been hypothesized that the presence of mean convection is slowing down the MJO (Storch et al., 1988).

The propagation speed of the signal in the upper ocean is diagnosed to be slightly slower than in "all year" conditions, namely 3.9 m/s.

c) Northern Summer (MJJA) conditions

Similarly to the winter conditions, the summer signal appears more clearly than the "all year" signal. Maximum percentage of explained 850 mb zonal wind variance is more than 50% (Fig. 8). The signal is propagating from the North Equatorial Indian Ocean across Southern Asia along the ITCZ to South America. Maximum wind anomalies are more than 3 m/s.

The ACPs of the buoy data are given in the following table:

Position	parameter	q^1	q^2	maximum at day	explained variance
165°E	u	0.76	-0.08	1	6%
	v	-0.32	-0.06	22	10%
	z	1.1	-1.2	6	6%
140°W	u	0.35	-0.45	7	19%
	v	0.19	0.09	3	6%
	z	-4.5	-3.1	18	14%

The wind signal at 140°W is stronger in MJJA than in NDJF, but at 165°E the winter signal is considerably stronger than the summer signal. The phase speed of the wind signal in summer is as in "all year" conditions, but the estimated propagation in the ocean, 5.9 m/s, is faster in summer than in winter.

4. POP Analysis of the Buoy Data: Coupled Variability of Wind and Thermocline Depth

A POP analyses was performed of the 6-dimensional vector given by the two wind components and the thermocline depth at the two buoy positions: the analysis interval is from Dec. 25, 1986 until Nov. 11, 1989.

A band-pass filter is invoked to suppress day-to-day variability as well as annual and inter-annual variations: all variability on time scales above 240 days and below 20 days is deleted. Variability on time scales between 30 and 150 days is not affected, and in the intervals 20-30 days and 150-240 days a cosine shaped filter is used. With this filter the expected MJO signal and the oceanic Kelvin wave signal should be captured (Madden and Julian, 1971; McPhaden and Taft, 1988). As a byproduct of the filtering, the gaps in the data (Fig. 1) are filled by means of trigonometric interpolation. Due to prime factor restrictions of the time filter procedure, the first 12 days have been discarded also.

Note that the chances for a clear result are marginal only: the time series are not very long in terms of the time scale of the oceanic Kelvin waves, gaps are large in the wind data (Fig. 1), and there is a full Cold Event (1988) and the end of a Warm Event (1986) included in the analysis interval.

One marginally useful POP is identified. Its period is 108 days with an e-folding time of 126 days. It explains 51% of the band-pass filtered variance. The results, apart from the e-folding time, are not sensitive to the details of the time filtering. The patterns are given in the following table, the typical temporal evolution is shown in Figure 9.

Position	parameter	q^1	q^2	maximum at day
165°E	u	0.32	1.13	5
	v	0.51	-0.20	33
	z	5.45	0.51	25
140°W	u	0.69	0.34	19
	v	-0.01	0.27	33
	z	0.26	-12.59	53

Thus, the ocean signal is identified as an amplifying eastward travelling wave with $z(140°W;t) \approx 2 \cdot z(165°E;t-28)$ and a phase speed of 6100 km/28 days = 2.5 m/s. The atmospheric signal, in terms of zonal wind, is also propagating eastward but it is damped: $u(140°W;t) \approx 0.5 \cdot u(165°E;t-14)$ with a speed of 6100 km/14 days = 5m/s. This phase speed is considerably too slow compared with the previously published results.

The strength of the signal in terms of the meridional wind (0.5 m/s) is only half of the strength of the zonal wind signal (1 m/s). Similarly to the finding in Section 3, the wind rotates anti-clockwise in the west but clockwise in the east.

The maximum of ocean signal at 165°E lags the maximum wind at that location by 20 days, or: $\partial_t z(165°E;t) \approx \alpha_{165} \cdot u(165°E;t+7)$ with $\alpha_{165} \approx 0.3$. At 140°W the depth is lagging the change of the wind: $\partial_t z(140°W;t) \approx \alpha_{140} \cdot u(140°W;t-7)$ with $\alpha_{140} \approx 1$.

If the depth anomalies are caused by local wind forcing, the z-signal should lag the wind signal by about 3 days which is the (frictional) time scale of the oceanic response to the wind forcing (using a viscosity of $10^{-2} m^2 s^{-1}$ and a thermocline depth of 150 m; McPhaden et al., 1988). At the eastern position, the lag doubles that time scales whereas at the western position the estimated lag has even reversed sign. The present numbers suggest an unreasonable setting namely that there is a strong atmospheric forcing at 140°W and that the resulting depth anomaly is radiating to the 165°E position.

The analysis of the POP coefficient time series (Fig. 10) yields the disappointing result that they are not significantly connected with the MJO index;

thus the MJO can not be accounted for the patterns identified. The cross spectral analysis of the POP coefficients (Fig. 11) indicates the presence of several time scales, namely above 100 days, 80 days and 40 days, on which the system oscillates.

To conclude: The POP analysis in its present form is not capable to describe reasonably and realistically the space-time characteristics of the two-buoy data set.

5. SUGGESTIONS

To get a better insight into the dynamical behavior of the intraseasonal variability of the atmosphere and ocean in the equatorial Pacific, it is suggested to fit a model made up by a combination the following ad-hoc equations:

$$z(140^\circ W;t) = \beta_z \cdot z(165^\circ E;t-\tau_z) + \text{memory}$$

$$u(140^\circ W;t) = \beta_u \cdot u(165^\circ E;t-\tau_u) + \text{memory}$$

$$\partial_t z(165^\circ E;t) = \alpha_{165} \cdot u(165^\circ E;t-\tau_{165}) + \text{memory}$$

$$\partial_t z(140^\circ E;t) = \alpha_{165} \cdot u(165^\circ E;t-\tau_{165}) + \text{memory}$$

An other possibility would be to extend the spatial degrees of freedom by including more data, e.g., the data from the 110°W mooring or sea level data.

Appendix

Normalization of ACPs with $\sqrt{2}$

References

Madden, R.A. and P. Julian, 1972: ....

McPhaden, M.J. and B.A. Taft, 1988: Dynamics of seasonal and intraseasonal variability in the eastern equatorial Pacific. - J. Phys. Oceano. 18, 1713-1732

McPhaden, M.J.; H.P. Freitag; S.P. Hayes and B.A. Taft, 1988: The response of the equatorial Pacific Ocean to a westerly wind burst in May 1986.- J. Geophys. Res. 93, 10589-10603

McPhaden et al., 1990

McPhaden and Hayes, 1990

Spillane, M.C.; D.B. Enfield and J.S. Allen, 1987: Intraseasonal oscillations in sea level along the west coast of the Americas. - J. Phys. Oceano. 17, 313-325

Storch et al., 1988: JGR

Storch and Xu, 1990: Climate Dynamics

Wunsch, Gill, Deep sea Res. 23

Figure Captions

Figure 1
Time series of surface wind (zonal and meridional component; m/s) and of 20°C isotherm (m) at 140°W and at 165°E.

Figure 2
The POPs (Principal Oscillation Patterns), q^1 and q^2, of the MJO signal in terms of equatorial velocity potential at 200 mbar. The POP coefficients develop such that the patterns tend to appear in the following characteristic sequence: ... → q^2 → q^1 → $-q^2$ → $-q^1$ → q^2 →... (From Storch and Xu, 1990).

Figure 3
The MJO-associated correlation patterns (ACPs), q^1 and q^2, of 850 mb zonal wind derived from May 1984 until April 1988 daily ECMWF analyses ("all year conditions"). Top: percentage of band pass variance explained by the MJO-ACPs.

Figure 4
The MJO-associated correlation patterns (ACPs), q^1 and q^2, of the surface wind at the two buoy locations. The straight lines indicate the ACPs, the ellipses the reconstructed temporal evolutions. The ticks are 1.5 days apart from each other.

Figure 5
The reconstructed MJO-ACP evolution of the 20°C isotherm depth at the two buoys.

Figure 6
Auto correlation function of band-pass filtered 20°C isotherm depth at 165°E and at 140°W.

Figure 7
Same as Figure 3, but for the winter (NDJF) subset of analyses.

Figure 8
Same as Figure 3, but for the summer (MJJA) subset of analyses.

Figure 9

POP reconstructed variations in the tropical Pacific at two buoy locations. Dashed: 140°W, solid: 165°E. Bottom: zonal wind; middle: meridional wind; top: 20°C isotherm depth.

Figure 10

Coefficients of the buoy data POPs shown in Fig. 9. Note that for a considerably portion of the entire time interval, wind data were missing (Fig.1). The Fourier band-pass filtering performed prior to the POP analysis lead to an interpolation of the data.

Figure 11

Cross spectral analysis of the two time series shown in Fig. 10

Fig 1

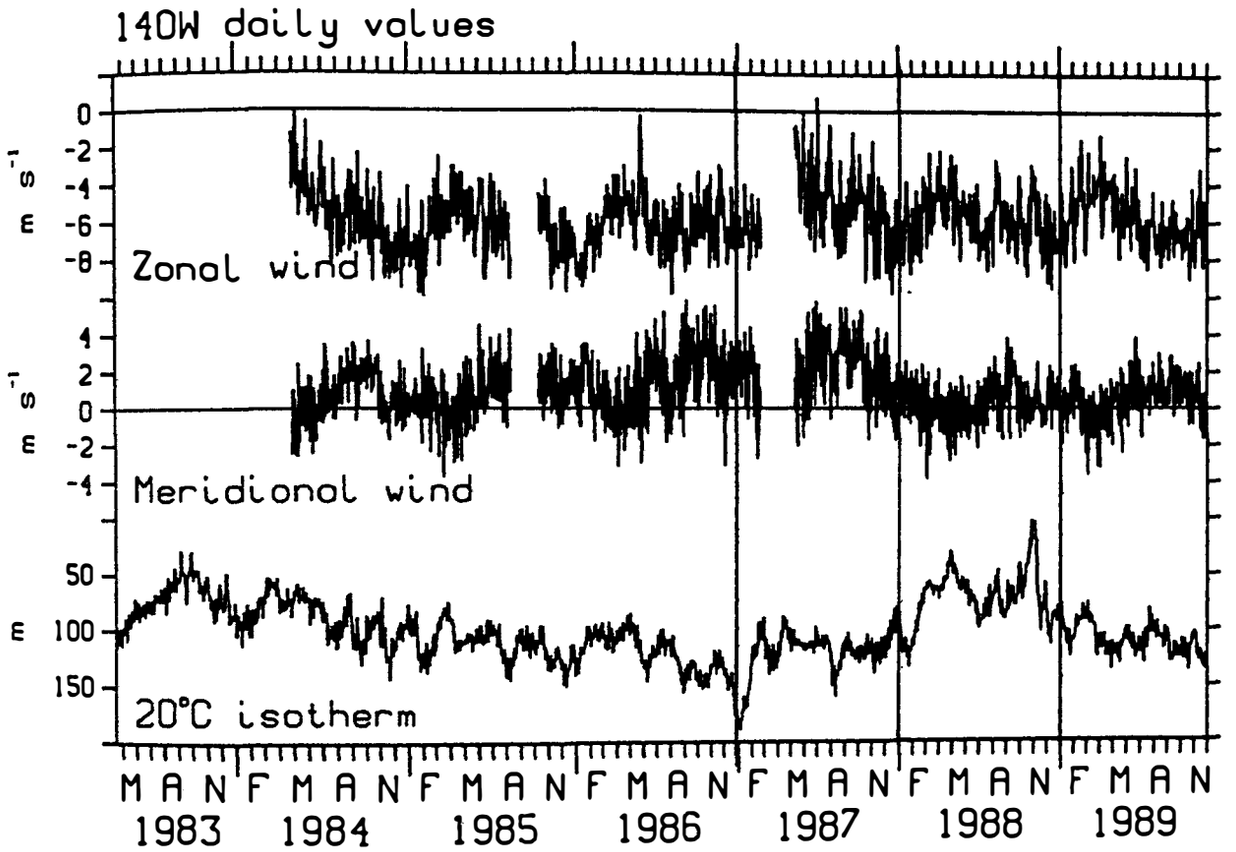
140W daily values
0
-2
-4
-6
-8
m s-1
Zonal wind
4
2
0
-2
-4
m s-1
Meridional wind
50
100
150
m
20°C isotherm
M A N F M A N F M A N F M A N F M A N F M A N F M A N
1983 1984 1985 1986 1987 1988 1989

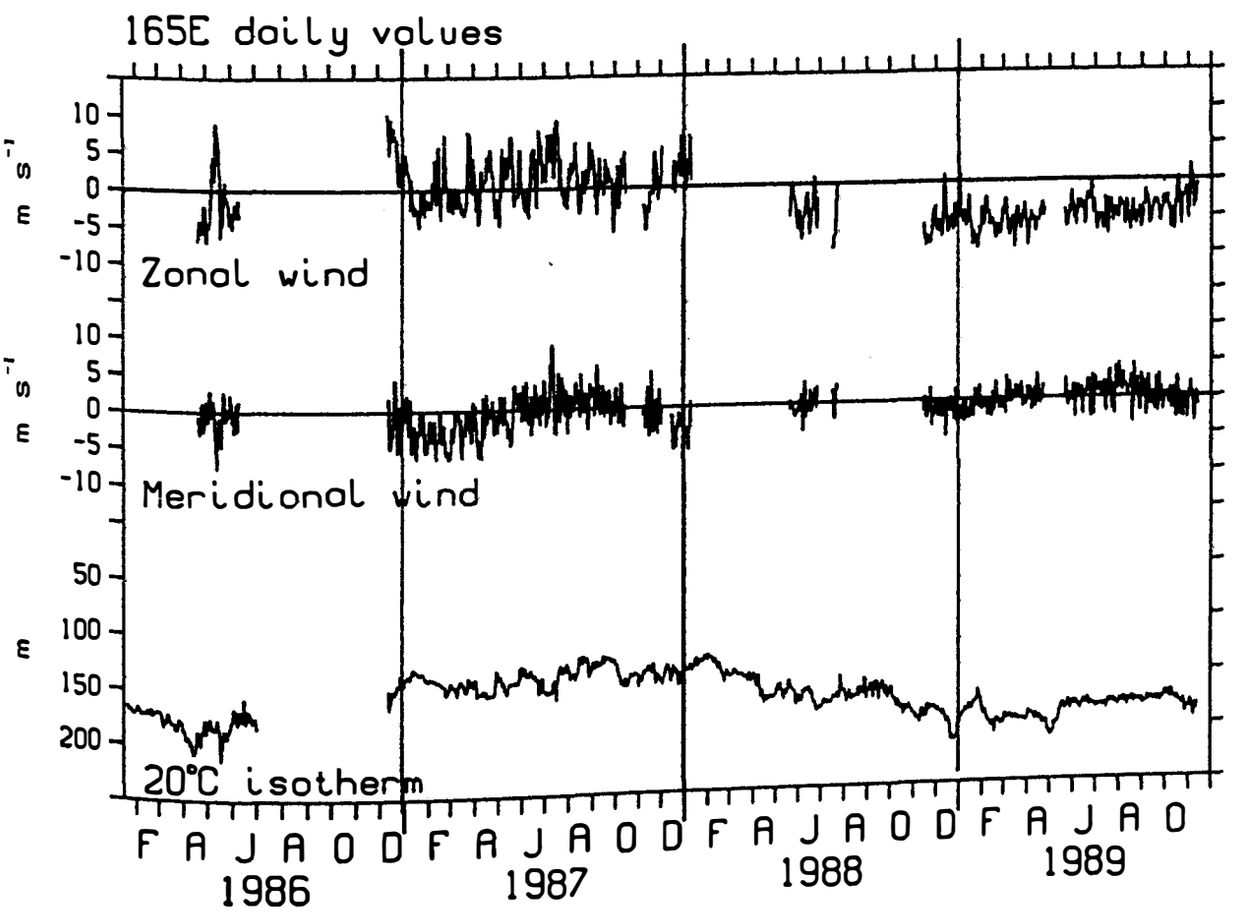
165E daily values
10
5
0
-5
-10
m s-1
Zonal wind
10
5
0
-5
-10
m s-1
Meridional wind
50
100
150
200
m
20°C isotherm
F A J A O D F A J A O D F A J A O D F A J A O
1986 1987 1988 1989

Fig. 2

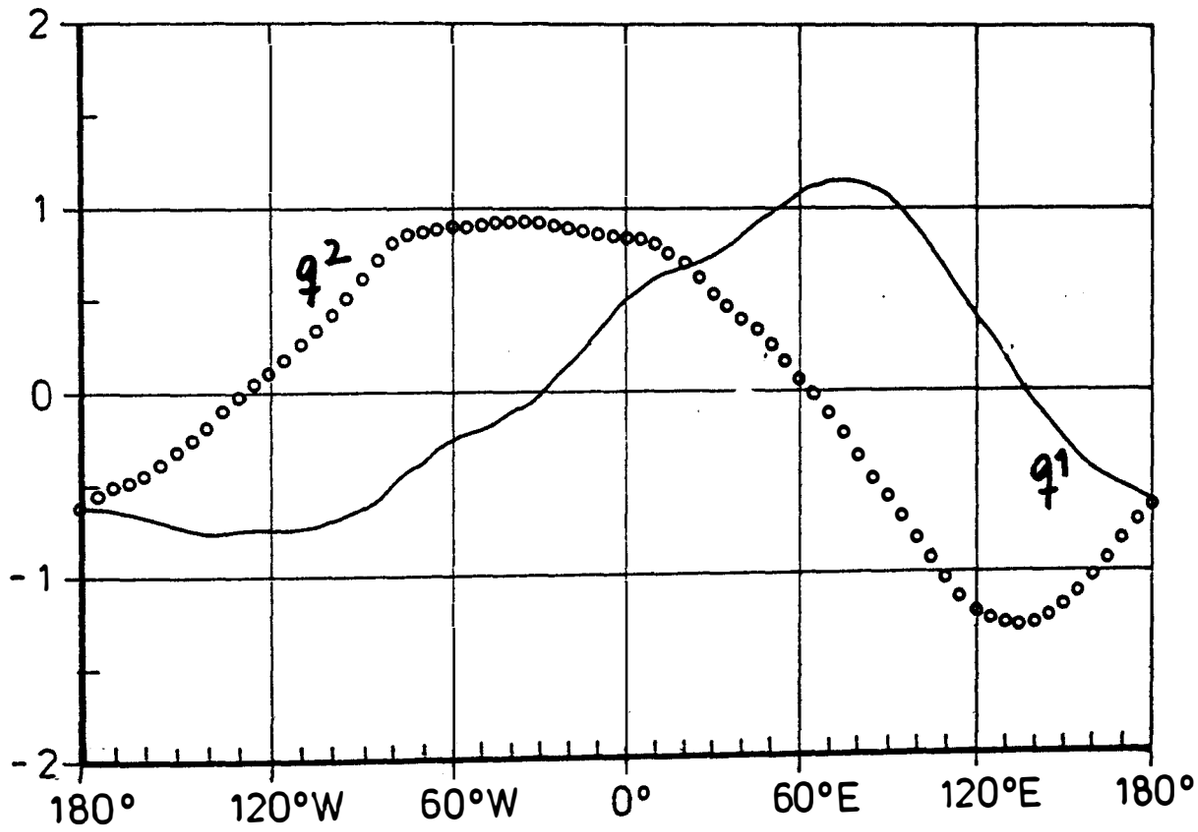

SAH660

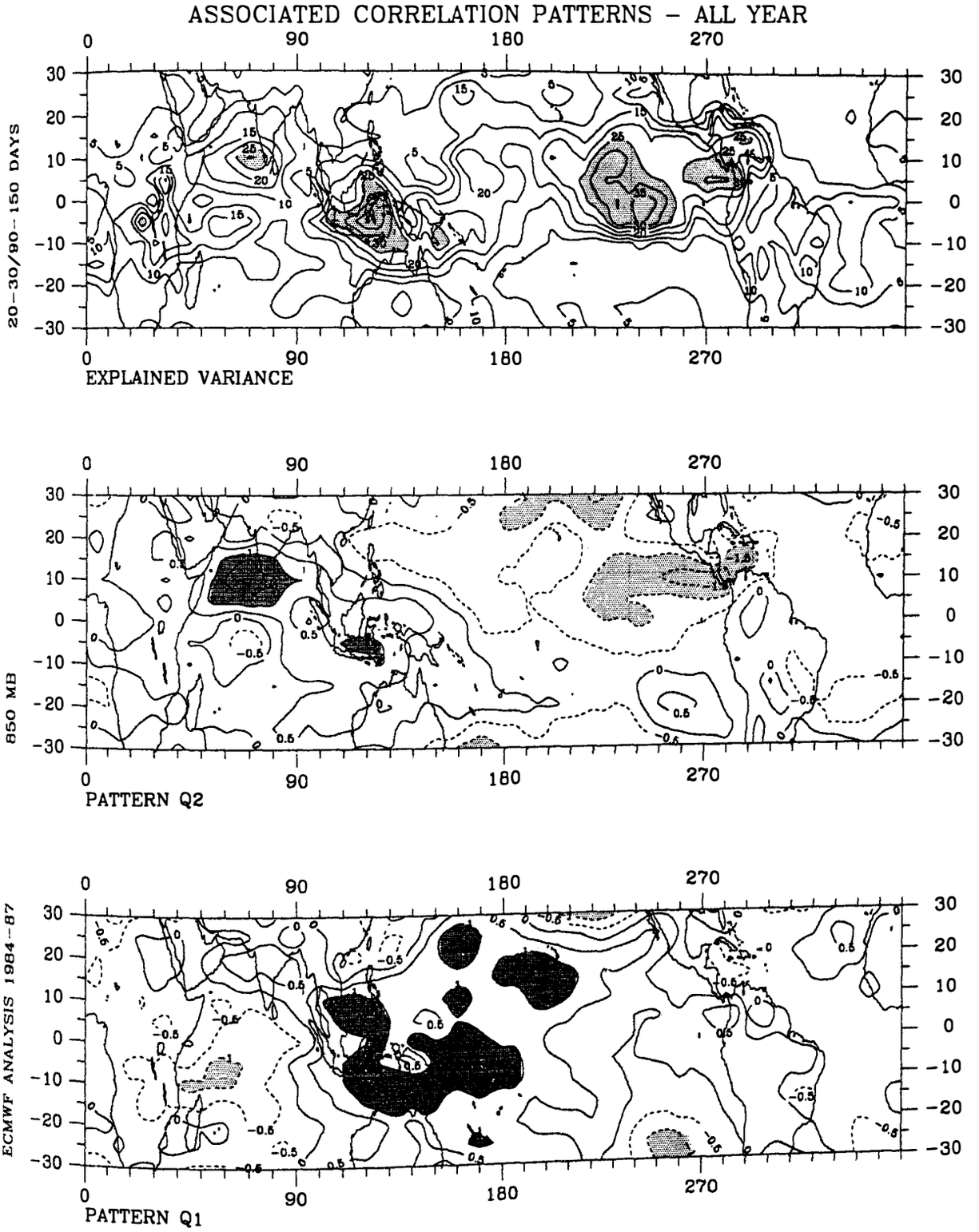
ASSOCIATED CORRELATION PATTERNS – ALL YEAR
20–30/90–150 DAYS
EXPLAINED VARIANCE
850 MB
PATTERN Q2
ECMWF ANALYSIS 1984–87
PATTERN Q1
0
90
180
270
30
20
10
0
-10
-20
-30

Fig 3.

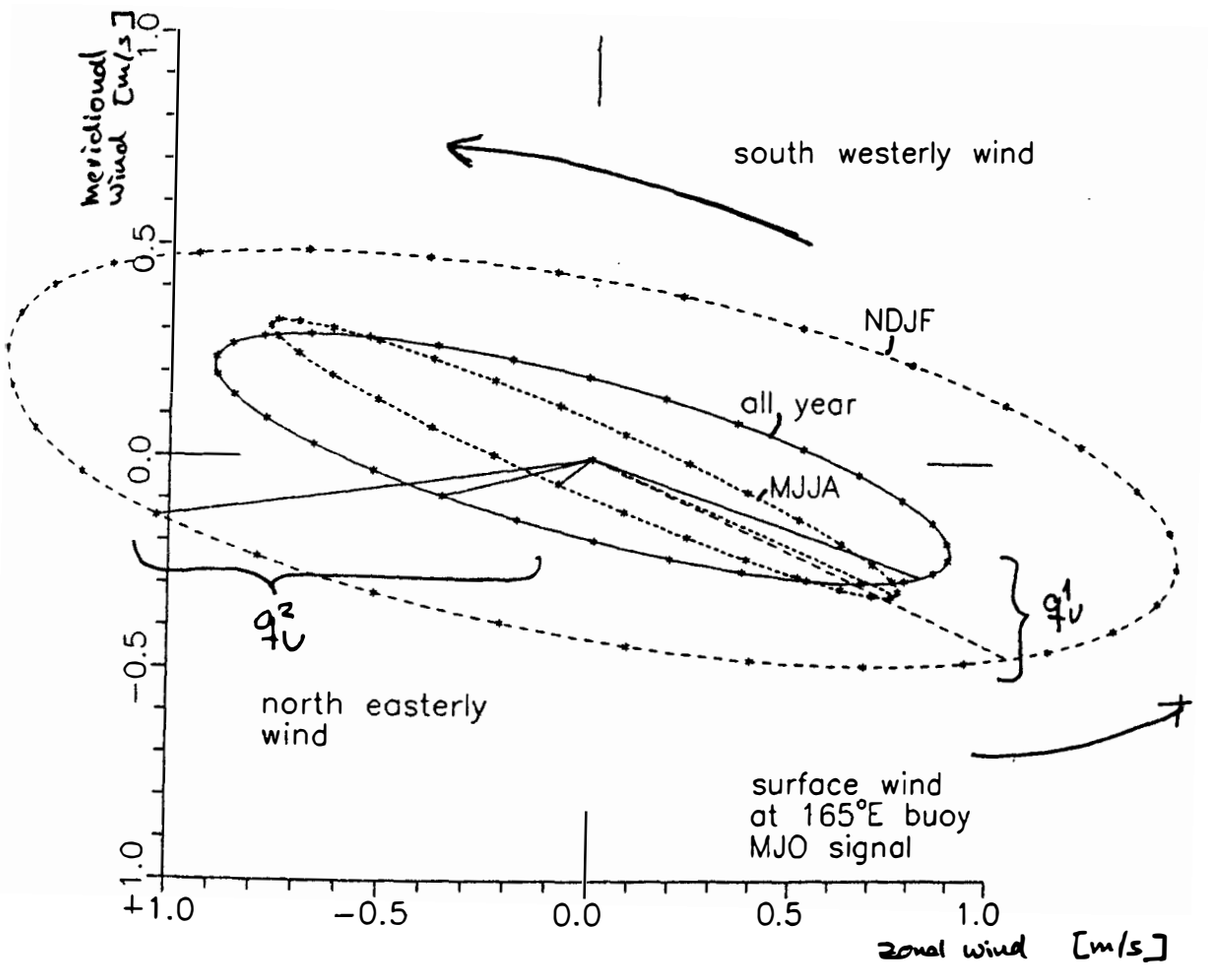
meridional wind [m/s]
1.0
0.5
0.0
−0.5
−1.0
south westerly wind
NDJF
all year
MJJA
q^2_U
q^1_U
north easterly wind
surface wind at 165°E buoy MJO signal
+1.0
−0.5
0.0
0.5
1.0
zonal wind [m/s]

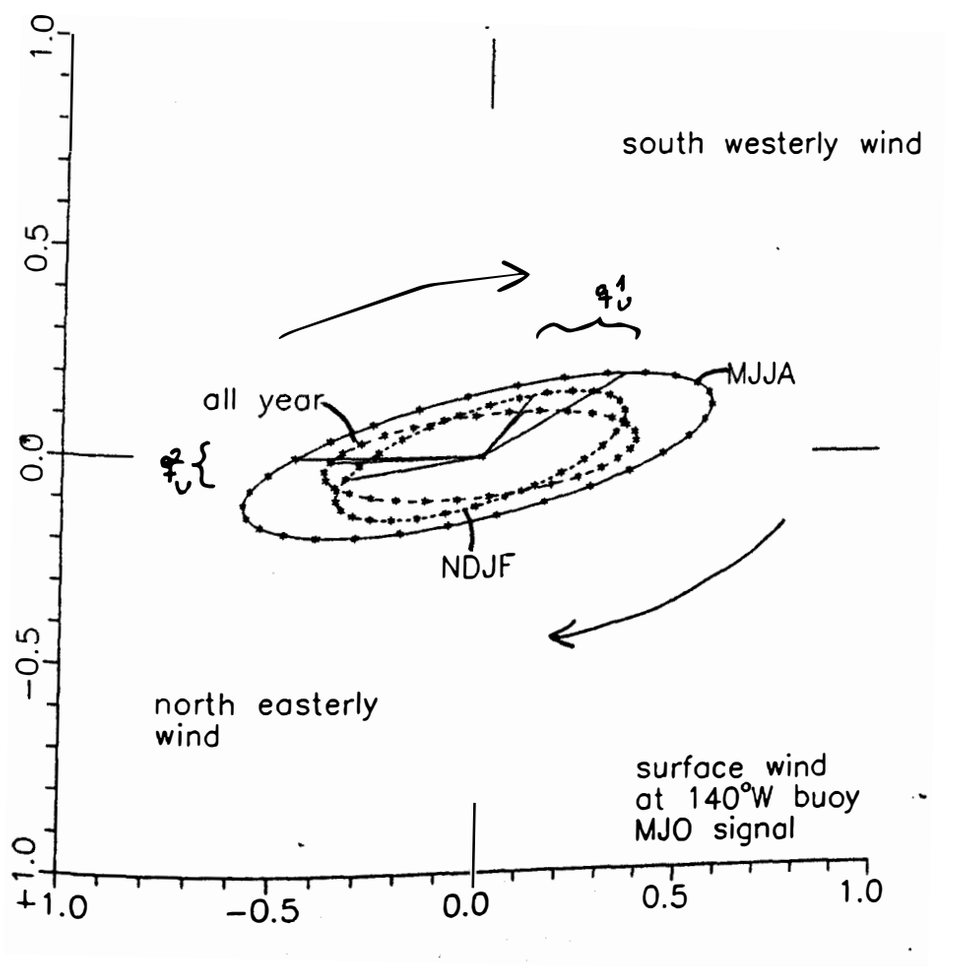
1.0
0.5
0.0
−0.5
−1.0
south westerly wind
q^1_U
MJJA
all year
q^2_U
NDJF
north easterly wind
surface wind at 140°W buoy MJO signal
+1.0
−0.5
0.0
0.5
1.0

Fig. 4

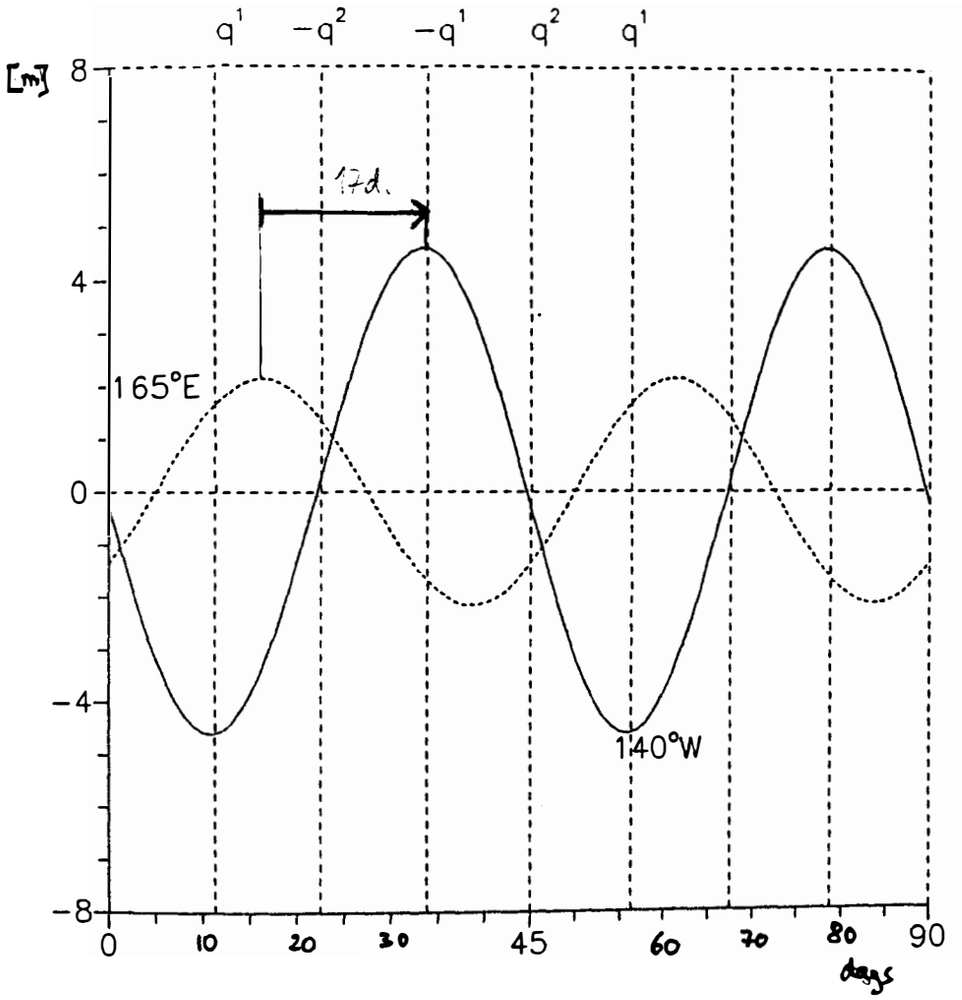

all year conditions
synthesized evolution
of 20°C isotherm depth

Fig 5

zsin.bas/
HvS 9/9/

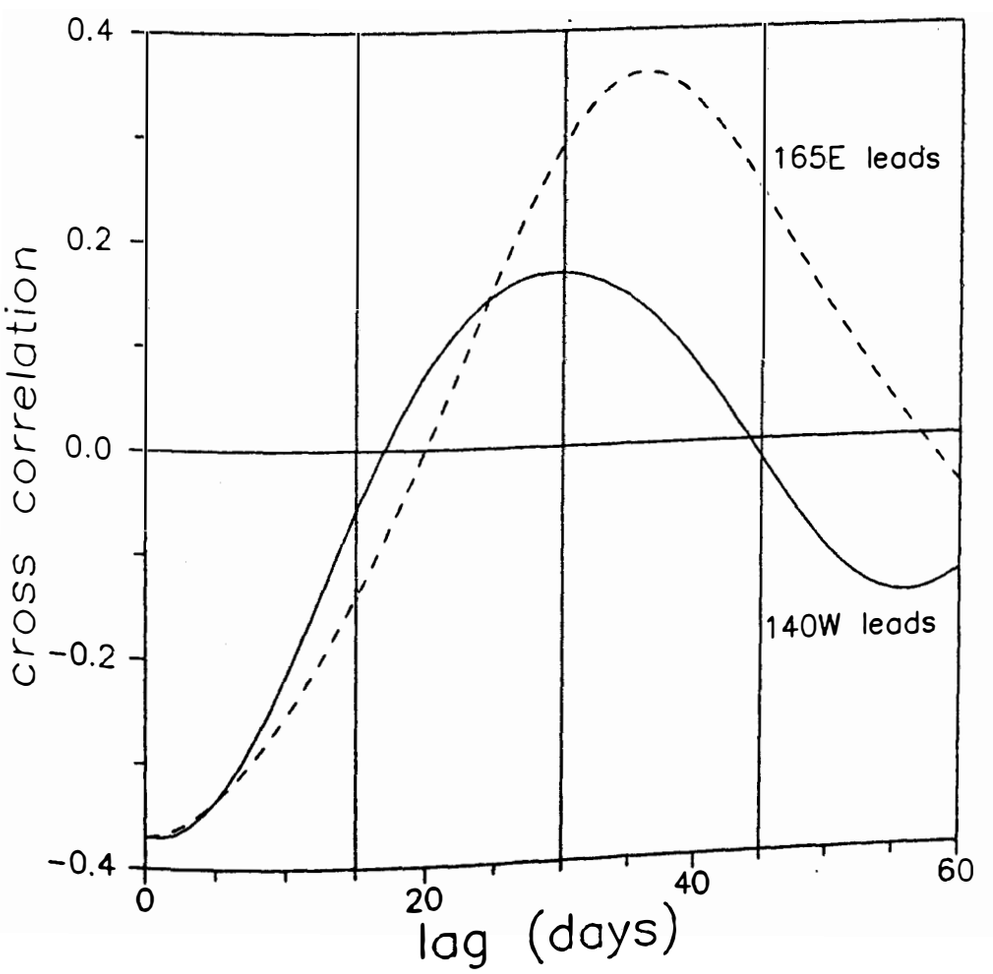

Data: depth of 20°C isotherm
at two equatorial buoys
band pass filtered (20–30/90–120)
approx. 1000 daily observations each
HvS, 7/9/1990

Fig 6

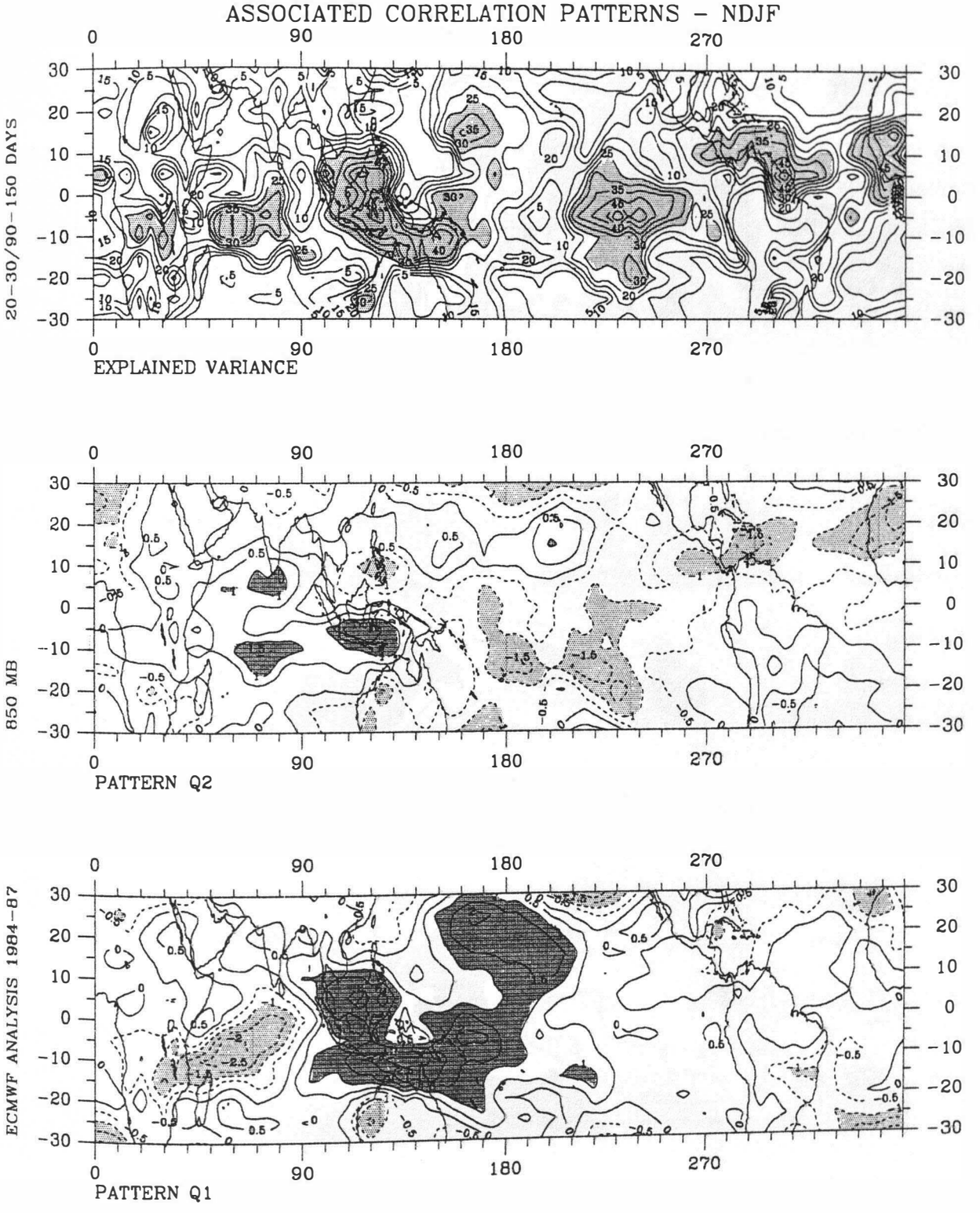
ASSOCIATED CORRELATION PATTERNS – NDJF
20–30/90–150 DAYS
EXPLAINED VARIANCE
850 MB
PATTERN Q2
ECMWF ANALYSIS 1984–87
PATTERN Q1
0
90
180
270
30
20
10
0
-10
-20
-30

Fig 7

Fig. 9

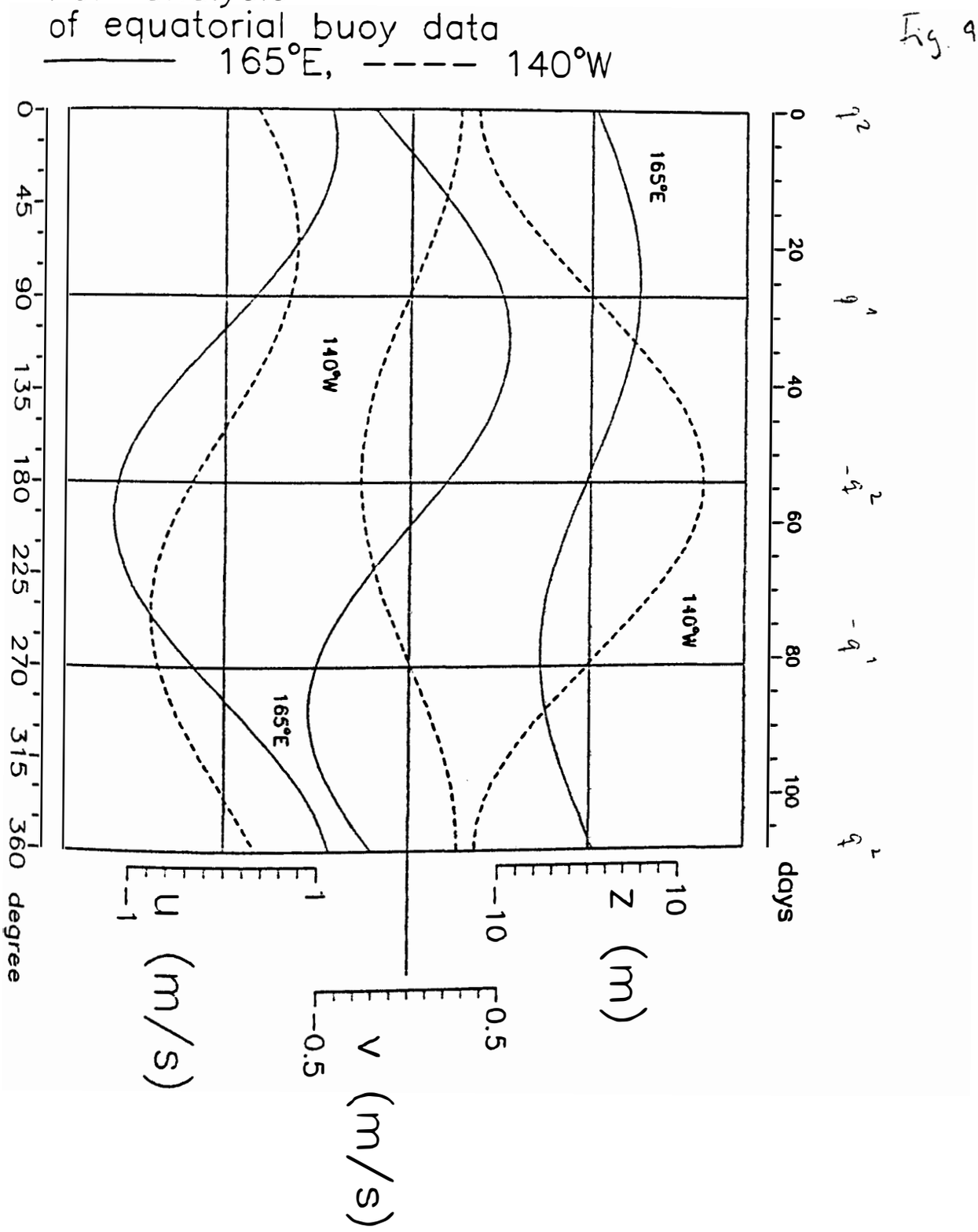

HvS 10/9/1990 poppha/popsin : 20–30/150–180 OFF

McPhaden data

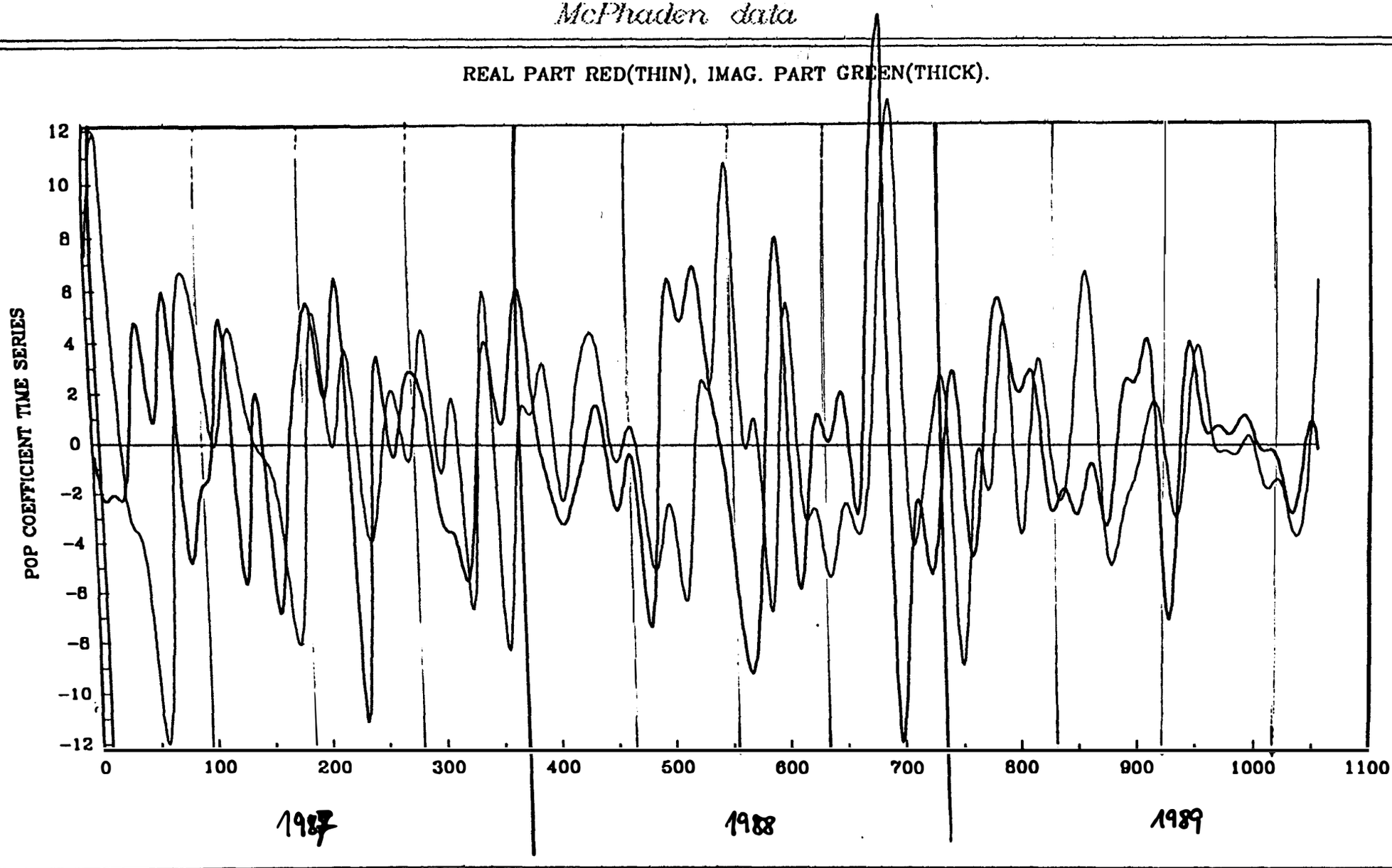

Comments: POP # 1/ 2 E-FOLDING TIME = 125.9 OSCILLATION PERIOD = 108.1
FILTER: 20/ 30 - 150/ 180,TREND-FILTERED.

DATE: 9/10/90 TIME: 17:40:49

Fig. 10.

Fig 11

McPhaden data

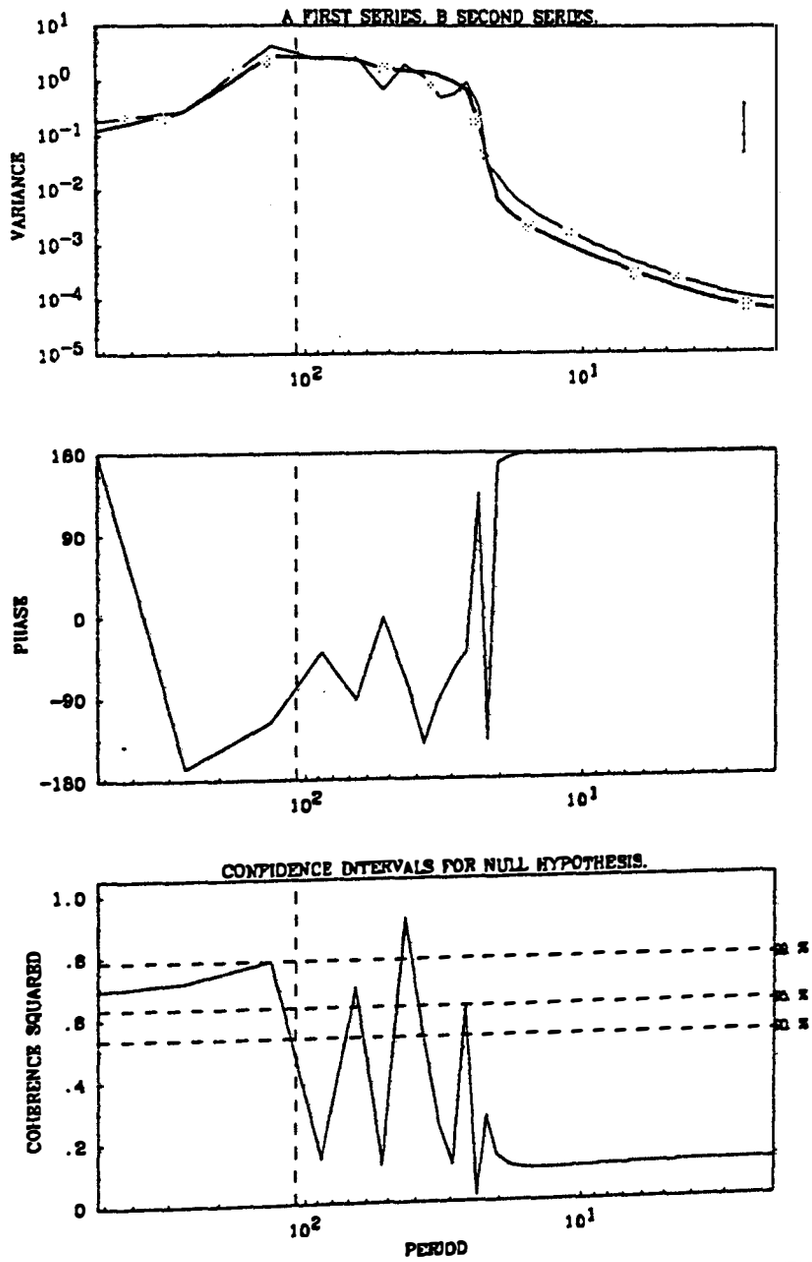

Comments: POP # 1/ 2 E-FOLDING TIME = 125.9 OSCILLATION PERIOD = 108.1
FILTER 20/ 30 - 150/ 180,TREND-FILTERED.

DATE: 9/10/80 TIME: 17:40:51

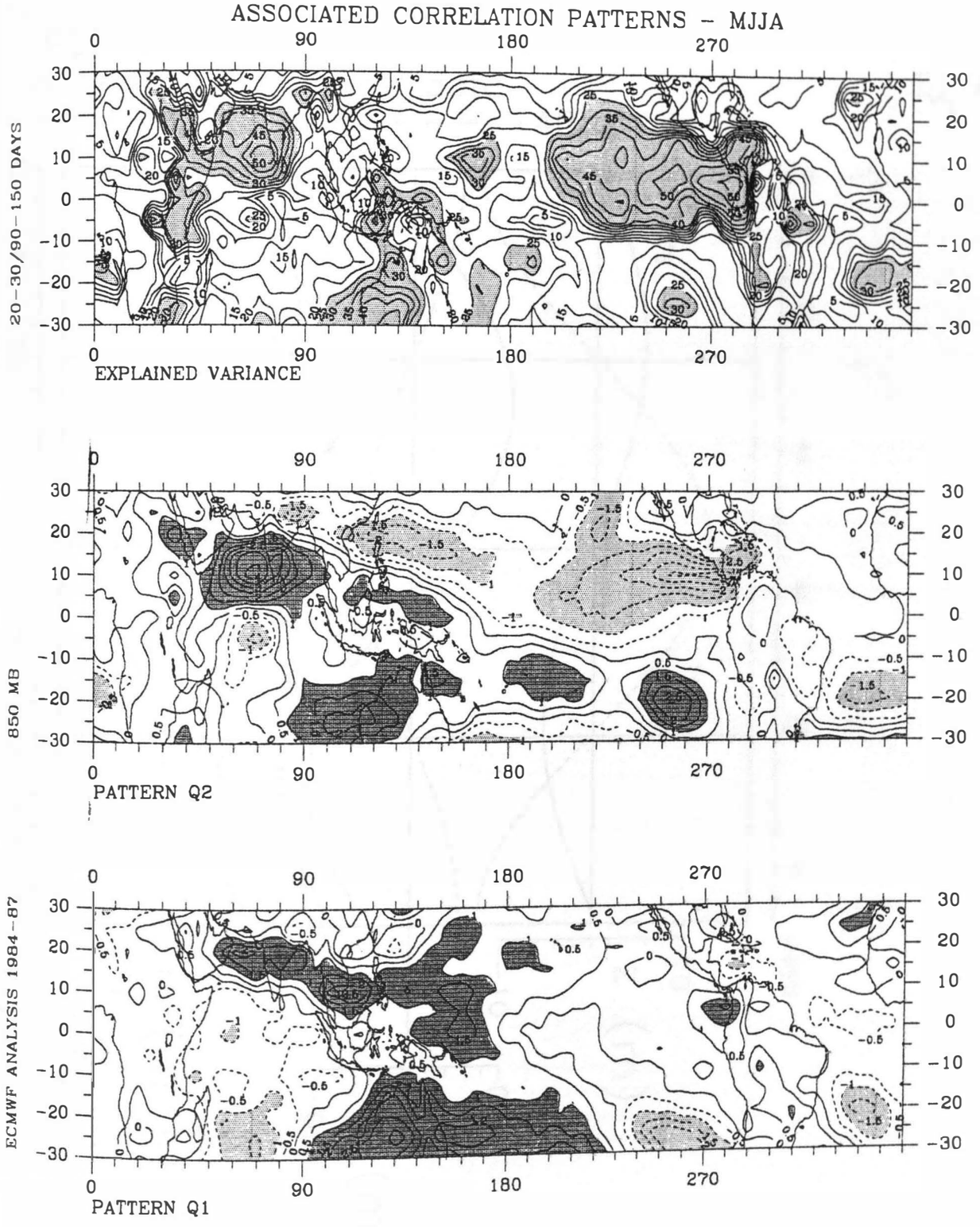
ASSOCIATED CORRELATION PATTERNS - MJJA
20-30/90-150 DAYS
EXPLAINED VARIANCE
850 MB
PATTERN Q2
ECMWF ANALYSIS 1984-87
PATTERN Q1
0
90
180
270
30
20
10
0
-10
-20
-30

Fig. 8